Contents lists available at GrowingScience

International Journal of Industrial Engineering Computations

homepage: www.GrowingScience.com/ijiec

Optimization for bi-objective express transportation network design under multiple topological structures

Jian Zhong[a], Xu Wang[a*], Longxiao Li[b] and Sergio García[c]

[a]*College of mechanical and vehicle engineering, Chongqing university, China*
[b]*School of business administration, Chongqing University of Science and Technology, China*
[c]*School of mathematics, University of Edinburgh, United Kingdom*

C H R O N I C L E

Article history:
Received December 10 2022
Accepted February 16 2023
Available online
February, 16 2023

Keywords:
Express transportation network design
Multiple topological structures
Bi-objective optimization

A B S T R A C T

With the rapid development of the courier industry, customers are placing higher demands on the cost and delivery time of courier services. Therefore, this paper focuses on the bi-objective express transportation network design problem (BO-ETNDP) to minimize the operation cost and maximum arrival time. A multi-structure parallel design methodology (MS-PDM) is proposed to solve the BO-ETNDP. In this methodology, all topological structures commonly used in designing transportation networks are sorted out. For each topological structure, a novel bi-objective nonlinear mixed-integer optimization model for BO-ETNDP is developed considering the impact of the hub's sorting efficiency on the operation cost and arrival time. To solve these models, a preference-based multi-objective algorithm (PB-MOA) is devised, which embeds the branch-and-cut algorithm and Pareto dominance theory in the framework of this ranking algorithm. In the case study, the applicability of the proposed methodology is verified in a real-world leading express company. The results show that our methodology can effectively avoid the limitation of solving the BO-ETNDP with a specific structure. Besides, the suitable topology for designing express transportation networks in different scenarios are explored through the sensitivity analysis.

1. Introduction

The courier industry, as an important support for the internet economy, has been in a rapid development stage. Despite the outbreak of the epidemic in 2020, the Chinese courier industry continues to grow rapidly. According to data released by the State Post Bureau of China, in 2020, the courier industry completed a total of 83.36 billion pieces of business for the year, up 31.2% year-on-year, with revenues exceeding 150.54 billion dollars, up 17.3% year-on-year. However, throughout 2020, China's courier industry received 716 complaints, of which 28.21% expressed customers' dissatisfaction about the long delivery time. Therefore, how to improve the timeliness of express logistics services is a challenge faced by courier companies. Currently, courier companies have taken positive actions. They are trying to improve the efficiency of the express transportation network (ETN). Real, Contreras, Cordeau, de Camargo, and de Miranda (2021) pointed out that optimizing the structure of the express transportation network plays an important role in improving the efficiency of ETNs, and an efficient ETN will help courier companies gain a huge advantage in the market competition. However, courier companies still lack a systematic and scientific theoretical approach to help them design an efficient ETN. Therefore, this paper focuses on the bi-objective express transportation network design problem (BO-ETNDP), where we seek to minimize the operation cost and the maximum arrival time. In the extant research, there are seven topologies commonly used in transportation network design, which can be divided into three categories. The first category is the fully connected (FC) structure, which is also known as point-to-point structure. FC structure makes a direct connection between each origin-destination (OD) pair. The second category is the hub-spoke structure that contains the single-allocation (SAHS), multi-allocation (MAHS), and R-allocation

* Corresponding author
E-mail: wx921@163.com (X. Wang)
ISSN 1923-2934 (Online) - ISSN 1923-2926 (Print)
2023 Growing Science Ltd.
doi: 10.5267/j.ijiec.2023.2.003

(RAHS) strategy. Hubs are special nodes on a network that concentrate shipments from their origins and redistribute them towards their destinations, hence benefitting the network from an economy of scale. Different allocation strategies imply the number of times a non-hub point can be allocated to a hub point and they are explained in Section 2. The third category is the hybrid structure combining the point-to-point and the hub-spoke structure. These topologies are shown in Fig. 1.

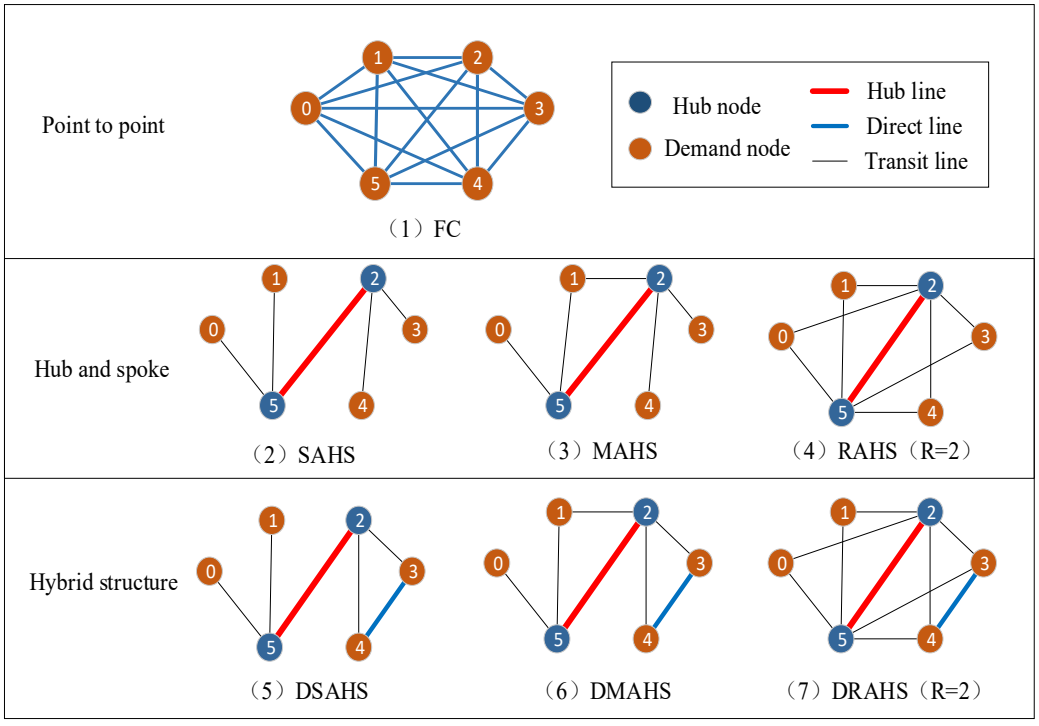

Fig. 1. Topologies commonly used in transportation network design.

Since different courier companies have different market sizes, the benefits of designing ETNs based on different topologies are unequal. For example, if a courier company has a very low business volume and it chooses a point-to-point structure to design ETNs, it will cause huge waste. If the business volume of a courier enterprise is very large, it is not necessary to choose the hub and spoke structure to design the ETN. Choosing different topologies for designing ETNs will affect the performance of ETNs in terms of operating cost and maximum arrival time. It is necessary to propose a reasonable method to select the appropriate topology for them to optimize ETNs. Therefore, two issues need to be clarified when designing ETNs.

(1) For courier companies with different business volumes, how to choose the appropriate topology to design an ETN with the lowest operation cost and shortest maximum arrival time?
(2) As business volumes and other market factors change, how to adjust the structure of ETNs to remain the lowest operation cost and shortest maximal arrival times?

To answer the two questions, this paper addresses the BO-ETNDP under multiple topological structures. To the best of our knowledge, few studies comprehensively consider the impact of topological structure on the performance of ETNs (see the literature review in Section 2). A multi-structure parallel design methodology (MS-PDM) is proposed here. In this methodology, all topological structures commonly used in designing transportation networks are sorted out. For each topological structure, a novel bi-objective nonlinear mixed-integer optimization model for BO-ETNDP is developed, which considers the impact of the hub's sorting efficiency on the operation cost and arrival time. In the courier industry, the sorting efficiency of the hub is an important decision variable. There is no relevant optimization model that makes the sorting efficiency of hubs as a decision variable to design ETNs. To solve these models, a preference-based multi-objective algorithm (PB-MOA) is devised. The main contributions of this paper are:

(1) This paper proposes a comprehensive multi-structure parallel design methodology to solve the BO-ETNDP, which can effectively avoid the limitation of solving the BO-ETNDP with a specific structure.
(2) For each topological structure, a novel multi-objective nonlinear mixed-integer optimization model for BO-ETNDP is developed. This model considers the impact of the hub's sorting efficiency on the operation cost and arrival time.
(3) This paper devises a preference-based multi-objective algorithm (PB-MOEA) for solving the bi-objective nonlinear mixed-integer optimization model, which can obtain high-quality feasible solutions and accurately measure its gap by comparing it with the lower bound.
(4) This paper verifies the applicability of this methodology to a leading express courier company and provides some valuable

managerial implications through the sensitivity analysis.

The remainder of this paper is organized as follows. Section 2 reviews relevant studies. The methodology for solving the BO-ETNDP is shown in Section 3. Section 4 presents the optimization models and PB-MOEA. In Section 5, case studies are presented to verify the performance of the proposed methodology. Some conclusions and future research are discussed in Section 6.

2. Literature review

From the perspective of transportation network design, the related literature on transportation network design can be divided into two categories. One is based on a specific network structure to design transportation networks, and the other is based on multiple network structures. To avoid the limitation of cost and timeliness of the transportation network designed based on a single network structure, this paper solves the BO-ETNDP under multiple network structure, that is, all potential network structures are considered. To this end, we have summed up all topological structures used in designing transportation networks. Firstly is the FC structure, which was developed by Aykin (1995), who noted that the goods between any two points can only be directly transported. Secondly is the single-allocation hub-and-spoke (SAHS), where a non-hub node must be allocated to one hub (ME, 1986). The third type is the multi-allocation hub-and-spoke (MAHS), which indicates that non-hub nodes can be allocated to multiple hubs (Campbell, 1992). The fourth type is the r-allocation hub-and-spoke (RAHS), which limits the number of connections between the non-hub nodes and the hub (Yaman, 2011). Besides, Aykin (1994) proposed a new idea of also allowing connections between non-hub nodes, thus forming the direct-connected single-allocation hub-and-spoke structure (DSAHS), the direct-connected multi-allocation hub-and-spoke structure (DMAHS), and the direct-connection r-allocation hub-and-spoke structure (DRAHS). These topological structures are widely used in the design of transportation networks, such as ocean transportation networks (Hsu & Hsieh, 2007; Ng & Kee, 2008; Tagawa, Kawasaki, & Hanaoka, 2021), air transportation networks (Bryan & O'Kelly, 2010; Erdemir, Batta, Rogerson, Blatt, & Flanigan, 2010), cargo transportation networks (Shang, Yang, Jia, Gao, & Ji, 2021; Yaman, Kara, & Tansel, 2007), hazmat network design (Taslimi, Batta, & Kwon, 2017). In addition, some other uncommon topological structures can be seen in other review articles (S. Alumur & Kara, 2008; S. A. Alumur et al., 2021; Batta, Lejeune, & Prasad, 2014; Farahani, Hekmatfar, Arabani, & Nikbakhsh, 2013; Gelareh & Nickel, 2011). For the purpose of our research, there are seven topologies commonly used in transportation network design and those are the ones that we will consider in this paper.

Few studies have comprehensively considered these seven different topologies when designing transportation networks. Most studies focus on one or a limited number of these topological structures. Hsu and Hsieh (2005) developed an optimization model for the ocean transportation network design with the FC and SAHS structures and determined the final solution by comparing the performance of transportation cost and inventory cost. Likewise, Imai, Shintani, and Papadimitriou (2009) designed the ocean transportation network considering container recycling. Notteboom, Parola, and Satta (2019) paid more attention to the flow changes in the final solutions. Recently, Tagawa et al. (2021) proposed a more comprehensive evaluation system to choose the final solution. Also, the topological structure derived from the hub-and-spoke structure is a hot spot. Ernst (2009) built mathematical models for transportation network design with SAHS and MAHS structures. Yaman (2011) devised an optimization model for designing transportation networks with RAHS structure. Tofighian and Arshadi khamseh (2020) also developed transportation network design models with SAHS and MAHS structures. Taherkhani and Alumur (2019) built an integer programming model for the transportation network design problems under the structure of SAHS, MAHS, RAHS and they also modelled the cases where direct connections between non-hub nodes are allowed. Although these studies are pioneering in transportation network design, a more comprehensive study of the impact of topology is still lacking.

In addition to the impact of the topological structure on the design of transportation networks, the sorting efficiency of the hub is an important decision variable in the courier industry. Higher sorting efficiency reduces the time spent on sorting packages in the hub, but with that comes a higher cost from purchasing sorting equipment. The operation cost and arrival times of packages are significantly affected by the sorting efficiency.

To the best of our knowledge, there is no relevant literature that makes the sorting efficiency of hubs a decision variable when designing transportation networks. da Graça Costa, Captivo, and Clímaco (2008) designed an SAHS transportation network with minimum operation costs and a minimized maximum service time, but they considered the sorting efficiency of hub stations as a parameter to construct an approximate function of the hub station's maximum service time instead of taking the sorting efficiency as a decision variable to comprehensively investigate the impact between the sorting efficiency and the operation cost. Ghodratnama, Tavakkoli-Moghaddam, and Azaron (2015) focused on the single-allocation hub location problem with the objective of minimizing costs and the service time, as well as greenhouse gas emissions. Likewise, they simply took the sorting efficiency of the hub station as a parameter, and only considered the impact between the sorting efficiency and the service time. Although Mohammadi, Tavakkoli-Moghaddam, Siadat, and Rahimi (2016) proposed an efficient algorithm to solve the bi-objective single allocation p-hub center-median problem under uncertainty, but ignored the impact of the sorting efficiency on the construct cost. Also, Lin, Zhao, and Lin (2020) and Karimi-Mamaghan, Mohammadi, Pirayesh, Karimi-Mamaghan, and Irani (2020) ignored the impact of the sorting efficiency on the construction cost of the hub. Shang et al. (2021) also took the sorting efficiency of the hub station as a parameter to address a bi-objective hierarchical

multimodal hub location problem.

The method of modeling transportation network design problems can be traced back to the 1990s. O'Kelly (1987) proposed a quadratic discrete optimization model for the hub location problem. However, due to the difficulty of solving this model, a path-based method was proposed by Skorin-Kapov, Skorin-Kapov, and O'Kelly (1996), who built a hub location model, and obtained tight linear programming relaxation bounds. The model involves a large number of variables $O(n^4)$ and constraints $O(n^3)$. Followed by them, other methods reducing the complexity of model variables and constraints are proposed. Ebery (Ebery, 2001) presented the first mixed integer linear program for solving single allocation hub location problems that requires only $O(n^2)$ variables and $O(n^2)$ constraints. de Camargo, de Miranda, and Ferreira (2011) introduced Benders reformulations to solve single allocation HLPs considering hub congestion costs. García, S., et al. (2012) first proposed a formulation with $O(n^2)$ to solve the multiple allocation p-hub location problem. Some other linearization strategies are used to deal with the quadratic discrete optimization model have achieved good results (An, Zhang, & Zeng, 2015; Azizi, Chauhan, Salhi, & Vidyarthi, 2016; Rostami, Kämmerling, Naoum-Sawaya, Buchheim, & Clausen, 2021; Sherali & Smith, 2007). In this paper, we have also adopted the path-based method to develop our optimization model for BO-ETNDP.

Although the extant studies have yielded significant results in transportation network design (S. A. Alumur et al., 2021), there are still some areas where further improvements can be made. Firstly, existing research focuses on one or several specific topologies to design ETN, and few studies comprehensively consider the impact of topological structure on the performance of ETN. Secondly, the sorting efficiency of the hub is an important decision variable for the courier industry while it is unreasonable to simply consider it as a parameter. Thirdly, few studies have analyzed the impact of sorting efficiency at hubs on the timeliness of courier services. To the best of our knowledge, no existing studies have integrated these factors into the transportation network design.

3. Problem description and methodology

A typical scenario of BO-ETNDP is considered. There are n demand nodes, each of which is a candidate hub station. Besides, there is demand for transporting some commodity between each pair of demand nodes. Considering these transportation demands can be large or small, two types of vehicles with different capacities are available. In actual operation, vehicles with large capacity are given priority to meet transportation demands. However, if the loading rate is too low, it will be more economical to choose vehicles with small capacity to transport.

BO-ETNDP aims to find an optimal solution with minimum operation costs and a minimum maximum arrival time. The optimal solution found provides insights into where to locate the hubs, how to design the sorting efficiency of hubs, how to connect hubs and demand nodes, and how to route flows.

Some constraints need to be included. Firstly, the most basic constraint is that each transportation demand must be satisfied. Secondly, once the package arrives at the hub, it must be dispatched within the company's specified hold time. Thirdly, the topology between hub stations is non-fully connected. Finally, the topology of the non-hub nodes needs to satisfy the constraints of the allocation strategy.

For the convenience of modeling, we make some assumptions which are common in the literature of BO-ETNDP. (1) After all packages at a hub are sorted, they can be transported to the next hub or demand node. (2) When sorting operations are performed at a hub, the hub follows the first-come-first-sorting principle. (3) The number of docks at a hub is sufficient regardless of the queue time of vehicles waiting for an empty dock. It implies that BO-ETNDP is unconstrained in capacity of hubs.

3.2 Multi-structure parallel design methodology

To solve the BO-ETNDP, we propose an optimization method called multi-structure parallel design methodology (MS-PDM). As mentioned in the literature review, we sort out seven types of topological structures commonly used in ETN design. For each topology, a mathematical model of BO-ETNDP is developed. Then we devise an efficient PB-MOEA to solve the seven models. Finally, we determine the final solution for BO-ETNDP by comparing the performance of the seven optimal solutions in terms of operation costs and the maximum arrival time. Fig. 2 shows the framework of the MS-PDM, which contains four layers. The input layer provides the data required for solving the BO-ETNDP, including demand data, geographic data, parameter setting data, and decision makers' preference data. The detailed introduction of these data is described in Section 4. In the model layer, mathematical models for the BO-ETNDP under different topological structures are constructed. These topological structures include FC, SAHS, MAHS, RAHS, DSAHS, DMAHS, DRAHS. In the algorithm layer, we devise an efficient PB-MOEA to solve these models. The PB-MOEA embeds a branch-and-cut algorithm, and Pareto dominance theory in the framework of this ranking algorithm, which ensures a high-quality solution. In the output layer, we select the final solution from the seven optimal solutions according to the decision-maker's preference.

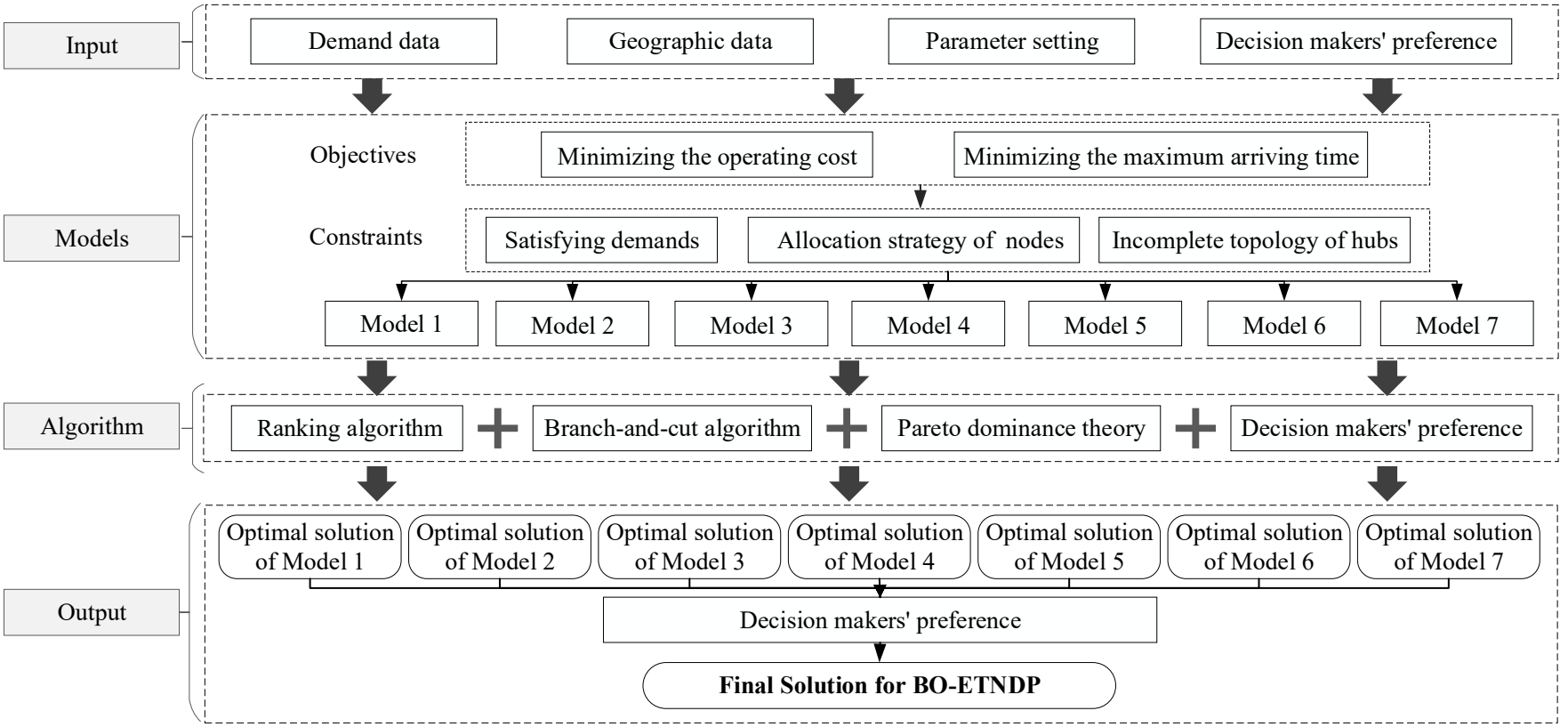

Fig. 2. Framework of the MS-PDM

4. Models and algorithms in MS-PDM

In this section, we first define the parameters used in MS-PDM, and then introduce the objective functions of operation costs and the maximum arrival time, followed by the mathematical models for BO-ETNDP under different topologies. Last, the PB-MOEA is introduced.

4.1 Parameters definition

To make the mathematical model clearer, we categorize the notation used in the model and algorithms and display them in Table 1.

Table 1
Definition of symbols

Set	Descriptions
N	Set of nodes, N=$\{1, \dots, n\}$
H	Set of candidate hubs, $H \subset N$, H=$\{1, \dots, k\}$
M	Set of vehicle types, M=$\{1, \dots, m\}$
Parameter	**Descriptions**
w_{ij}	Demand flow from node $i \in N$ to node $j \in N$
d_{ij}	Length of the arc between nodes $i \in N$ and $j \in N$
c_m	Transportation cost per kilometer for the mth type vehicle, $m \in M$
q_m	Capacity of the mth type vehicle, $m \in M$
mc_m	Monthly fixed cost of the mth type vehicle, $m \in M$
FH_k	Monthly fixed cost of the kth hub, $k \in H$
FD_i	Monthly fixed cost of the ith node, $i \in N$
lt	Departure time of vehicles leaving the node
dt	Company-defined hold time for packages in the hub
s	The service time spent by vehicles in a hub
ε	The unit cost for improving the sorting efficiency in a node
$d\varepsilon$	The unit cost discount for improving the sorting efficiency in a hub
θ	The unit cost for sorting packages in a node
$d\theta$	The unit cost discount for sorting packages in a hub
v	The speed of the vehicle in km/h
p_c	Preference coefficient of operation costs
p_t	Preference coefficient of the maximum arrival time
Decision Variable	**Descriptions**
e_k	Integer, the sorting efficiency of hub k (pieces/hour)
f_{ikl}	Integer, number of packages sent from node $i \in N$ that pass through hubs $k \in H$ and $l \in H$
X_{ik}	Binary, equals 1 if node i is assigned to hub $k \in H$ and 0 otherwise
Y_{ijkl}	Binary, equals 1 if parcels of node $i \in N$ sent to node $j \in N$ pass through hubs $k \in H$ and $l \in H$ and 0 otherwise
Z_{kl}	Binary, equals 1 if an inter-hub link is operating from hub $k \in H$ to hub $l \in H$ and 0 otherwise
S_{ij}	Binary, equals 1 if there is a direct connection from non-hub node $i \in N$ to non-hub node $j \in N$ and 0 otherwise

4.2 Bi-objective function

To ensure the good performance of the ETN in terms of cost and timeliness, we consider two objective functions in the optimization model of BO-ETNDP: minimizing operation costs and minimizing the maximum arrival time.

4.2.1 Operation cost function

Since the composition of operation cost in ETNs designed with different topologies is different (Serper & Alumur, 2016), we divide the operation cost function into three categories.

(1) Operation cost in the model of BO-ETNDP with FC structure

The operation cost OC_0 in the model of BO-ETNDP with the FC structure is composed of five parts, as shown in equation (1): monthly fixed cost of nodes (FN_0), fixed cost of opening the transportation line (FL_0) between any two nodes (opening the transportation line requires to buy a certain number of vehicles to meet the transport demands, which means that the cost of opening a transportation line is represented by the cost of purchasing vehicles), fixed cost (FS_0) for purchasing the sorting equipment, transportation cost (TS_0), and sorting cost of packages (SC_0). Among them, the calculation formulas of these costs are shown in (1.1)-(1.5). By $\lceil x \rceil$ we represent the smallest integer greater than or equal to x.

$$OC_0 := FN_0 + FL_0 + FS_0 + TS_0 + SC_0 \tag{1}$$

$$FN_0 := \sum_{i \in N} FD_i \tag{1.1}$$

$$FL_0 := \sum_{i \in N} \sum_{j \in N} \left\lceil \frac{w_{ij}}{q_m} \right\rceil * mc_m * S_{ij} \tag{1.2}$$

$$FS_0 := \sum_{i \in N} e_i * \varepsilon \tag{1.3}$$

$$TS_0 := \sum_{i \in N} \sum_{j \in N} c_m * d_{ij} * \left\lceil \frac{w_{ij}}{q_m} \right\rceil * S_{ij} \tag{1.4}$$

$$SC_0 := \sum_{i \in N} \sum_{j \in N} w_{ij} * \theta \tag{1.5}$$

(2) Operation cost in the model of BO-ETNDP with SAHS, MAHS, RAHS structure

The operation cost OC_1 in the model of BO-ETNDP with SAHS, MAHS, or RAHS structure is also composed of five parts, as shown in equation (2): monthly fixed cost of hubs and nodes (FN_1), fixed cost of opening the transportation line (FL_1) which includes opening the transportation line between two hubs and the transportation line between a hub and a node, fixed cost (FS_0) for purchasing the sorting equipment (if there is a large amount of sorting work at the hubs, economies of scale can be formed, so the unit cost discount for improving the sorting efficiency in the hub is considered), transportation cost (TS_0), and sorting cost of packages (SC_0). Among them, the calculation formulas of these costs are shown in (2.1)-(2.5).

$$OC_1 := FN_1 + FL_1 + FS_1 + TS_1 + SC_1 \tag{2}$$

$$FN_1 := \sum_{k \in H} FH_k X_{kk} + \sum_{i \in N} FD_i \tag{2.1}$$

$$FL_1 := \sum_{k \in H} \sum_{l \in H} \left\lceil \frac{\sum_{i \in N} f_{ikl} + \sum_{i \in N} f_{ilk}}{q_m} \right\rceil * mc_m + \sum_{i \in N} \sum_{k \in H} \left\lceil \frac{\sum_{l \in H} f_{ikl}}{q_m} \right\rceil * mc_m \tag{2.2}$$

$$FS_1 := \sum_{k \in H} e_k * \varepsilon * d\varepsilon \tag{2.3}$$

$$TS_1 := \sum_{i \in N} \sum_{j \in N} \sum_{k \in H} \sum_{l \in H} (c_m d_{ik} + c_m d_{lj}) \left\lceil \frac{w_{ij}}{q_m} \right\rceil Y_{ijkl} + \sum_{k \in H} \sum_{L \in H} c_m d_{kl} \left\lceil \frac{\sum_{i \in N} f_{ikl}}{q_m} \right\rceil \tag{2.4}$$

$$SC_1 := \sum_{i \in N} \sum_{j \in N} w_{ij} * \theta * d\theta \tag{2.5}$$

(3) Operation cost in the model of BO-ETNDP with DSAHS, DMAHS, DRAHS structure

Likewise, the operation cost OC_2 in the model of BO-ETNDP with DSAHS, DMAHS, or DRAHS structure is composed of five parts, as shown in equation (3): monthly fixed cost of hubs and nodes (FN_2), fixed cost of opening the transportation line (FL_2) (includes opening the transportation line between two hubs, the transportation line between a hub and a node, and the direct line between two non-hub nodes), fixed cost for purchasing the sorting equipment (FS_2), transportation cost (TS_2), and sorting cost of packages (SC_2). Among them, the calculation formulas of these costs are shown in (3.1)-(3.5).

$$OC_2 := FN_2 + FL_2 + FS_2 + TS_2 + SC_2 \tag{3}$$

$$FN_2 := \sum_{k\in H} FH_k X_{kk} + \sum_{i\in N} FD_i \tag{3.1}$$

$$FL_2 := \sum_{k\in H}\sum_{l\in H}\left\lceil\frac{\sum_{i\in N} f_{ikl}+\sum_{i\in N} f_{ilk}}{q_m}\right\rceil * mc_m + \sum_{i\in N}\sum_{k\in H}\left\lceil\frac{\sum_{l\in H} f_{ikl}}{q_m}\right\rceil * mc_m + \sum_{i\in N}\sum_{j\in N}\left\lceil\frac{w_{ij}}{q_m}\right\rceil * mc_m * S_{ij} \tag{3.2}$$

$$FS_2 := \sum_{k\in H} e_k * \varepsilon * d\varepsilon + \sum_{i\in N}\sum_{j\in N} w_{ij} * \varepsilon * S_{ij} \tag{3.3}$$

$$TS_2 := \sum_{i\in N}\sum_{j\in N}\sum_{k\in H}\sum_{l\in H}(c_m d_{ik} + c_m d_{lj})\left\lceil\frac{w_{ij}}{q_m}\right\rceil Y_{ijkl} + \sum_{k\in H}\sum_{L\in H} c_m d_{kl}\left\lceil\frac{\sum_{i\in N} f_{ikl}}{q_m}\right\rceil + \sum_{i\in N}\sum_{j\in N}\left\lceil\frac{w_{ij}}{q_m}\right\rceil c_{ij} d_{ij} S_{ij}) \tag{3.4}$$

$$SC_2 := (\sum_{i\in N}\sum_{j\in N} w_{ij} - \sum_{i\in N}\sum_{j\in N} w_{ij} * S_{ij}) * \theta * d\theta * 2 + \sum_{i\in N}\sum_{j\in N} w_{ij} * S_{ij} * \theta \tag{3.5}$$

4.2.2 Arrival time function

To reduce the uncertainty of arrival time, the arrival time function is formulated based on the business process of express logistics services (Esmizadeh, Bashiri, Jahani, & Almada-Lobo, 2021; Zahiri & Suresh, 2021). Each component of the arrival time is then estimated based on historical data. Since the BO-ETNDP with different topological structures has different business processes, we divide the arrival time function into two categories.

(1) Arrival time in the model of BO-ETNDP with FC structure

The arrival time in the ETN designed with FC structure is composed of two parts, as shown in equation (4): the transportation time and the service time spent by the vehicle in node i.

$$at_{ij} := \frac{d_{ij}}{v} + s \quad \forall j \in N. \tag{4}$$

(2) Arrival time in the model of BO-ETNDP with another structures

According to the business process of express logistics services shown in Fig. 3, the arrival time in ETNs designed with SAHS, MAHS, RAHS, DSAHS, DMAHS, and DRAHS is composed of collection time, branch transportation time, primary sorting time, trunk transportation time, secondary sorting time, branch transportation time, and delivery time. Since the collection time and delivery time are related to the vehicle scheduling strategy and are not within the scope of the network design, this paper does not consider the collection time and the delivery time.

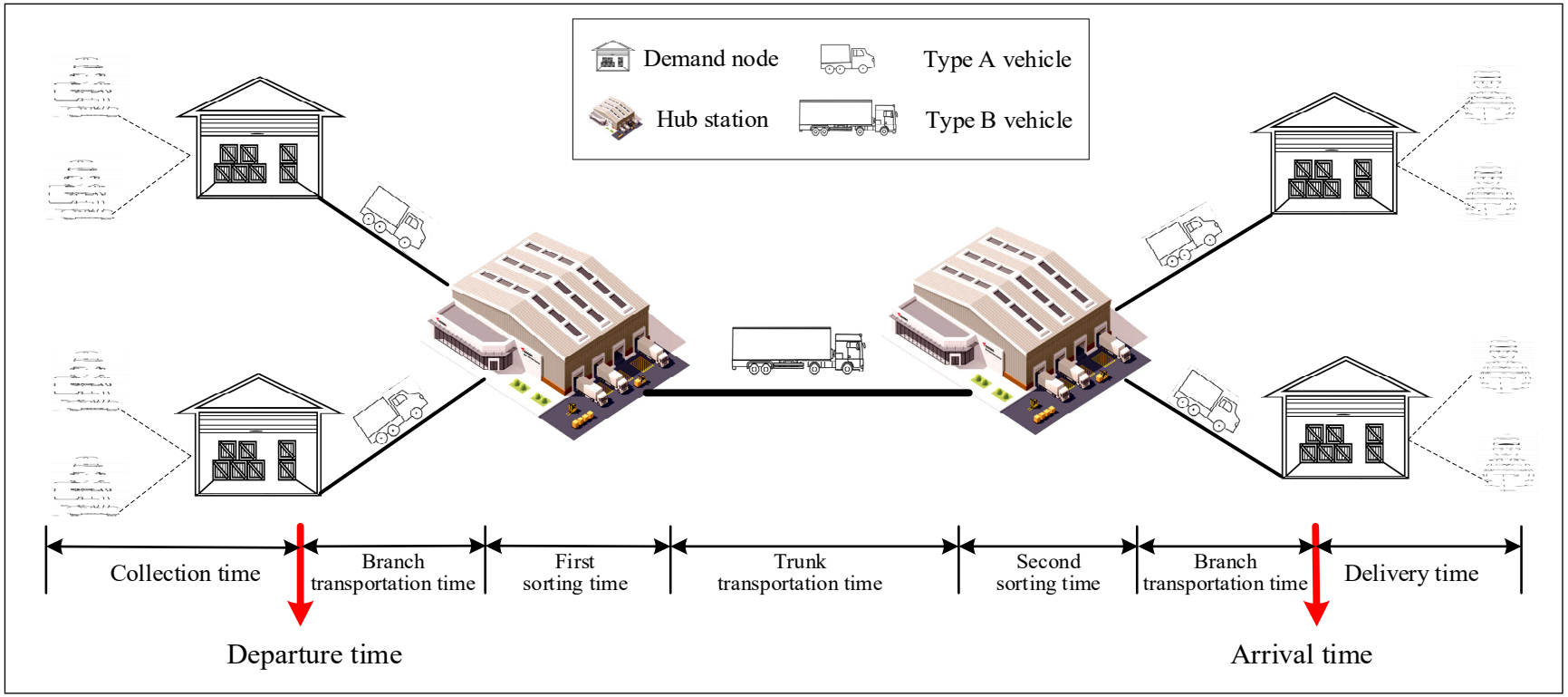

Fig. 3. The business process of the express logistics service

Table 2 shows the notation used to formulate the arrival time function.

Table 2

Definition of time in business process

Symbols	Definition
lt_i	Departure time of vehicles from node $i \in N$ to hub $k \in H$
bt_{ik}	Branch transportation time of vehicles from node $i \in N$ to hub $k \in H$
bt_{lj}	Branch transportation time of vehicles from hub $l \in H$ to node $j \in N$
ht_{kl}	Trunk transportation time of vehicles from hub $k \in H$ to hub $l \in H$
st_{ik}	Time of packages from node $i \in N$ start to be sorted in hub $k \in H$
et_k	End time when hub $k \in H$ completes all sorting tasks
st_{kl}	Time of packages from hub $k \in H$ start to be sorted in hub $l \in H$
et_l	End time when hub $l \in H$ completes all sorting tasks
hw_{ik}	Number of parcels in node $i \in N$ that are allocated to hub $k \in H$ for sorting
hw_{kl}	Number of parcels in hub $k \in H$ that are allocated to hub $l \in H$ for sorting

Then, we formulate the relationship between the parcel arrival time function at'_{ij} and the decision variables in formula (5) below:

$$at'_{ij} := \sum_{l \in H} et_l X_{jl} + bt_{lj} \quad \forall i, j \in N. \tag{5}$$

The relationship between bt_{lj} and decision variable X_{jl} is shown in (5.1). Besides, et_l is related to the start time of sorting packages in hub $l \in H$ and the time spent in the sorting process. As packages from other hubs do not arrive in hub $l \in H$ in the meantime, the end time of these packages sorted in hub $l \in H$ is different. Therefore, we set the longest time of these packages spent in hub $l \in H$ as et_l, which is calculated in (5.2).

$$bt_{lj} := \frac{\sum_{l \in H} d_{jl} X_{jl}}{v} \quad \forall j \in N \tag{5.1}$$

$$et_l := \max_{\forall k \in H} \{st_{kl} + hw_{kl}/e_l\} \quad \forall l \in H \tag{5.2}$$

The relationship between hw_{kl} and decision variables Y_{ijkl} is shown in (5.3). Since st_{kl} is related to s, their relationship is shown in (5.4).

$$hw_{kl} := \sum_{i \in N} \sum_{j \in N} w_{ij} Y_{ijkl} \quad \forall k, l \in H \tag{5.3}$$

$$st_{kl} := et_k + ht_{kl} + s \tag{5.4}$$

The relationship between ht_{kl} and decision variables Y_{ijkl} is described in (5.5). et_k is related to the start time of sorting packages in hub $k \in H$ and the time spent in the sorting process. Since the packages from other nodes do not arrive in hub $k \in H$ at the same time, the end time of these packages being sorted at hub $k \in H$ is different. Therefore, we set the longest time that these packages spend in hub $k \in H$ as et_k, which is shown in (5.6).

$$ht_{kl} := (\sum_{k \in H} \sum_{l \in H} d_{kl} Y_{ijkl})/v \quad \forall i, j \in N \tag{5.5}$$

$$et_k := \max_{\forall k \in H} \{ st_{ik} + hw_{ik}/e_k \} \tag{5.6}$$

The relationship between hw_{ik} and decision variables f_{ikl} is displayed in (5.7). Since st_{ik} is related to bt_{ik} and s, their

relationship is shown in (5.8).

$$hw_{ik} := \sum_{l\in H} f_{ikl} \quad \forall i \in N, k \in H \tag{5.7}$$
$$st_{ik} := bt_{ik} + \mathrm{s} \quad \forall i \in N \tag{5.8}$$

Then, we formulate the relationship between bt_{ik} and the decision variables X_{ik} as shown in (5.9).

$$bt_{ik} := (\sum_{k\in H} d_{ik} X_{ik})/v \quad \forall i \in N \tag{5.9}$$

Finally, the relationship between at'_{ij} and the decision variables is expressed in formula (6). These notations of formula (6) are same with the notations in the Table 1.

$$at'_{ij} := \sum_{l\in H} \max_{\forall k\in H} \left\{ \max_{\forall k\in H} \left\{ \frac{\sum_{k\in H} d_{ik} X_{ik}}{v} + \frac{\sum_{l\in H} f_{ikl}}{e_k} + s \right\} + \frac{\sum_{k\in H}\sum_{l\in H} d_{kl} Y_{ijkl}}{v} + \frac{\sum_{i\in N}\sum_{j\in N} w_{ij} Y_{ijkl}}{e_l} + s \right\} * X_{jl} + \frac{\sum_{l\in H} d_{jl} X_{jl}}{v} \quad \forall i, j \in N \tag{6}$$

4.3 Optimization models

In the MS-PDM, all topological structures commonly used in the design of ETN were sorted out. For each topological structure, a multi-objective nonlinear mixed-integer optimization model for BO-ETNDP is developed using a formulation based on path flows.

4.3.1 Model 1: ETND with FC structure

$$\min f_0 := OC_0 \tag{7}$$
$$\min f_1 := \max_{\forall i,j\in N} \{ at_{ij} \} \tag{8}$$

s.t.

$$S_{ij} = 1 \quad \forall i, j \in N \tag{9}$$
$$\sum_{j\in N} w_{ij}/e_i \le dt \quad \forall i \in N \tag{10}$$
$$S_{ij} \in \{0,1\} \quad \forall i, j \in N \tag{11}$$
$$e_i \ge 0 \quad \forall i \in N \tag{12}$$

In Model 1, objective function (7) minimizes the operation cost and objective function (8) minimizes the maximum arrival time. Constraint (9) ensures that the direct connections are operated between any two non-hub nodes. Constraint (10) enforces that the hold time of packages in the hubs observed. Constraint (11) and (12) represent the binary and non-negative variables.

4.3.2 Model 2: ETND with SAHS structure

$$\min f_1 := OC_1 \tag{13}$$
$$\min f_2 := \max_{\forall i,j\in N} \{ at'_{ij} \} \tag{14}$$

s.t.

$$\sum_{k\in H}\sum_{l\in H} Y_{ijkl} = 1 \quad \forall i, j \in N \tag{15}$$
$$\sum_{k\in H} X_{ik} = 1 \quad \forall i \in N \tag{16}$$
$$\sum_{l\in H} f_{ikl} - \sum_{l\in H} f_{ilk} = \sum_{j\in N}\sum_{l\in H} w_{ij} Y_{ijkl} - \sum_{j\in N}\sum_{l\in H} w_{ij} Y_{ijlk} \quad \forall i \in N, k \in H \tag{17}$$
$$(\sum_{l\in H}\sum_{i\in N} f_{ikl} + \sum_{l\in H}\sum_{i\in N} f_{ilk})/e_k \le rt \quad \forall k \in H \tag{18}$$

$$X_{ik} \leq X_{kk} \qquad \forall i \in N, k \in H \qquad (19)$$

$$Y_{ijkl} \leq X_{ik} \qquad \forall i, j \in N, k, l \in H \qquad (20)$$

$$Y_{ijkl} \leq X_{jl} \qquad \forall i, j \in N, k, l \in H \qquad (21)$$

$$Z_{kl} \leq X_{kk} \qquad \forall k, l \in H \qquad (22)$$

$$Z_{kl} \leq X_{ll} \qquad \forall k, l \in H \qquad (23)$$

$$Z_{kl} = \begin{cases} 1, \ \sum_{i \in N} \sum_{j \in N} Y_{ijkl} \geq 1 \\ 0, \ \sum_{i \in N} \sum_{j \in N} Y_{ijkl} = 0 \end{cases} \qquad \forall k, l \in H \qquad (24)$$

$$X_{ik} \in \{0,1\} \qquad \forall i \in N, k \in H \qquad (25)$$

$$Y_{ijlk} \in \{0,1\} \qquad \forall i, j \in N, k, l \in H \qquad (26)$$

$$e_k \geq 0 \qquad \forall k \in H \qquad (27)$$

$$f_{ikl} \geq 0 \qquad \forall i \in N, k, l \in H \qquad (28)$$

In Model 2, objective function (13) minimizes the operation cost and objective function (14) minimizes the maximum arrival time. Constraint (15) imposes that each demand between any two nodes is satisfied. Constraint (16) ensures that each non-hub node is assigned to a single hub. Constraint (17) is the flow balance equation. Constraint (18) enforces that the service time in a hub is satisfied within the maximum service time. Constraint (19) guarantees that the nodes are assigned only to installed hubs. Constraints (20) and (21) represent the allocation strategy of the link. Constraints (22) and (23) ensure that each inter-hub link is operated only in-between hubs. Constraint (24) indicates that if the path exists, the inter-hub link must be opened. Constraints (25) and (26) represent the binary variables. Constraints (27) and (28) represent the non-negative variables.

4.3.3 Model 3: ETND with MAHS structure

$$\min f_1 := OC_1 \qquad (13)$$

$$\text{Min } f_2 := \max_{\forall i,j \in N} \{ at'_{ij} \} \qquad (14)$$

s.t. (15), (17)-(28)

Objective functions of Model 3 and Model 2 are identical. Regarding the constraints, the only difference is that constraint (16) needs to be ignored in the ETND model with MAHS structure because each non-hub node can be assigned to multiple hubs in the MAHS structure.

4.3.4 Model 4: ETND with RAHS structure

$$\min \ f_1 := OC_1 \qquad (13)$$

$$\min f_2 := \max_{\forall i,j \in N} \{ at'_{ij} \} \qquad (14)$$

s.t. (15), (17)-(28)

$$\sum_{k \in H} X_{ik} \leq R \qquad \forall i \in N \qquad (29)$$

In Model 4, the objective functions are the same as in model 2 and model 3, which includes minimizing the operation cost (13) and the maximum arrival time (14). Regarding the constraints, the difference is that constraint (16) in Model 2 needs to

be modified as formula (29) because the number of hubs that can be allocated to each point is specified in the RAHS structure.

4.3.5 Model 5: ETND with DSAHS structure

$$\min f_1 := OC_2 \tag{30}$$
$$\min f_2 := \max_{\forall i,j \in N} \{ at'_{ij} \} \tag{14}$$
s.t. (16)-(18), (24)-(28)
$$S_{ij} + \sum_{k \in H} \sum_{l \in H} Y_{ijkl} = 1 \qquad \forall i,j \in N \tag{31}$$
$$S_{ij} + X_{ii} \leq 1 \qquad \forall j \in N,\ i \in H \cap N; \tag{32}$$
$$S_{ij} + X_{jj} \leq 1 \qquad \forall i \in N,\ j \in H \cap N; \tag{33}$$
$$S_{ij} \in \{0,1\} \qquad \forall i,j \in N \tag{34}$$

In Model 5, objective function (30) minimizes the operation cost and objective function (14) minimizes the maximum arrival time. The constraints are composed of (16)-(18), (24)-(28), (31)-(34). Constraint (31) derives from modifying constraint (15), which ensures that each demand between any two nodes is satisfied. Constraints (32) and (33) enforce that the direct links are opened only between non-hub nodes. Constraint (34) represents the binary variables.

4.3.6 Model 6: ETND with DMAHS structure

$$\text{Min } f_1 := OC_2 \tag{30}$$
$$\text{Min } f_2 := \max_{\forall i,j \in N} \{ at'_{ij} \} \tag{14}$$
s.t. (17), (18), (24)-(28), (31)-(34)

The objective functions of Model 6 and Model 5 are the same, which include objection function (30) and (14). Its constraints are composed of (17), (18), (24)-(28), (31)-(34).

4.3.7 Model 7: ETND with DRAHS structure

$$\min f_1 := OC_2 \tag{30}$$
$$\min f_2 := \max_{\forall i,j \in N} \{ at'_{ij} \} \tag{14}$$
s.t. (17), (18), (24)-(29), (31)-(34)

In Model 7, the objective functions are the same as in Model 5 and Model 6, which include minimizing the operation cost (30) and the maximum arrival time (14). The constraints are composed of (17), (18), (24)-(29), (31)-(34).

4.4 Preference-based multi-objective exact algorithm

Since objective function (14) is non-linear, these models are multi-objective non-linear mixed-integer optimization models (MO-NL-MIOM). To solve these models, we devise a method that we call PB-MOEA and stands for preference-based multi-objective algorithm. PB-MOEA embeds branch-and-cut algorithm in the framework of a ranking algorithm. In the ranking algorithm, for each objective, a preference value is specified by the decision-maker, and the objective with maximum preference value remains as the only objective of the model. In such a case, the branch-and-cut algorithm is applied to solve the single objective mixed-integer optimization model. Then, the optimal solution and a certain number of feasible solutions remain to construct the Pareto frontier. Finally, the optimal criterion constructed according to the decision-maker's preference is used to select an optimal solution from the Pareto frontier. To describe each step of the algorithm, we take Model 2 as example. Model 2 is an MO-NL-MIOM, and its mathematical expression is shown below in (35). In objective function f_1 we seek to minimize operation costs, and in f_2 we seek to minimize the maximum arrival time. Objective function f_2 is non-linear.

$$\begin{cases} \text{Min } \{ f_1, f_2 \} \\ s.t. \text{ Constraints } (15) - (28) \end{cases} \tag{35}$$

Then, we apply the PB-MOEA to solve the MO-NL-MIOM.

Step 1. Targets ranking

We rank the optimization targets according to the preferences of decision-makers. In this step, the importance of each goal is scored based on the decision-maker's experience of solving the MO-ETNDP. Then, we rank these targets based on the score. Regarding this problem, decision-makers usually prioritize the operation costs of express transportation networks.

Step 2. Model relaxation

Based on Step 1, the objective function with the maximum score is taken as the only objective of the original model. Thus, the multi-objective optimization model is relaxed to a single-objective optimization model. For Model 2, objective function f_1 has the maximum score, so we ignore objective function f_2. The relaxed model is shown in (36).

$$\begin{cases} \text{Min } f_1 \\ s.t. \text{ Constraints } (15)-(28) \end{cases} \tag{36}$$

Step 3. Solving the relaxed model

In this step, we use the branch-and-cut algorithm to solve the relaxed model. The optimal solution s_0 is obtained, and a certain number of feasible solutions s_i are collected for depicting the Pareto frontier. In this case, we keep all feasible solutions s_i within 10% gap of the optimal solution by setting the PoolGap parameter in Gurobi solver. Solutions that are not within the specified gap are discarded. Then, the solution set of the relaxed model is obtained, as shown below:

$$S \coloneqq \{s_0 \dots s_i \dots s_n\} \tag{37}$$

Step 4. Computing the value of each target in the original model

For each solution $s_i \in S$ of the relaxed model, we calculate its performance on targets f_1 and f_2. The value set of the target is expressed as follows:

$$F_1 \coloneqq \{f_1(s_0) \dots \dots f_1(s_n)\} \tag{38}$$

$$F_2 \coloneqq \{f_2(s_0) \dots \dots f_2(s_n)\} \tag{39}$$

Step 5. Depicting the Pareto frontier

In this step, we find all the non-dominated solutions from the feasible solution set *S* based on the Pareto dominance theory shown in (40). A ≺B represents that solution A dominates solution B, if and only if solution A is superior to or as good as solution B in all objectives or if there is at least one objective for which solution A is superior to solution B.

$$A \prec B \text{ if } (\ \forall o \in \{1,2\},\ f_o(A) \leqslant f_o(B)\ ) \wedge (\exists o \in \{1,2\} / f_o(A) < f_o(B)\ ) \tag{40}$$

Step 6. Obtaining the optimal solution on the Pareto frontier

In this step, we use the experience of decision-makers to select the optimal solution from the non-dominated solution set *P*, as shown in (41). $F(s_i)$ represents the deviation of the solution s_i, and the smaller the fitness, the higher the quality of the solution. The non-dominated solution with the minimum deviation is the optimal solution of the MO-NL-MIOM.

$$F(s_i) \coloneqq\ p_c * \frac{f_1(s_i)-\min\{F_1\}}{\max\{F_1\}-\min\{F_1\}} + p_t * \frac{f_2(s_i)-\min\{F_2\}}{\max\{F_2\}-\min\{F_2\}} \qquad \forall s_i \in P \tag{41}$$

Given the process of the PB-MOEA, we summarize the advantages of this algorithm for solving MO-NL-MIOMs. First, when the second objective function in the model has nonlinear characteristics, this algorithm can significantly improve efficiency. Besides, since we employ an accurate algorithm (branch-and-cut algorithm) to solve the relaxed model, we can accurately measure the optimality of each feasible solution by comparing it with the lower bound. Moreover, the decision-maker's practical experience is incorporated into the criteria of optimal solution selection, which allows the optimal solution to be filtered out with better applicability.

5. Case study

To verify the effectiveness of the proposed methodology, some case experiments are conducted in this section.

5.1 Data and Parameter setting

The data in this experiment is collected from a Chinese express company, as shown in Appendix Tables 1-3. We collected the company's data for a whole month during October 2020, which includes 34 demand nodes across the country, 6 candidate hub stations, and 1122 original-destination (OD) pairs. The distribution of demand nodes and candidate hub stations is shown in Figure 3. The red and black dots are demand nodes, and the black dots represent candidate hubs. Besides, the transportation flow among the 1122 OD pairs has significant imbalance characteristics, specifically including the imbalance in different regions and the round-trip OD pairs. China's manufacturing industries are concentrated in coastal cities, and the volume of parcels sent from coastal cities to the mainland is much larger than the volume of parcels sent from the mainland to coastal cities.

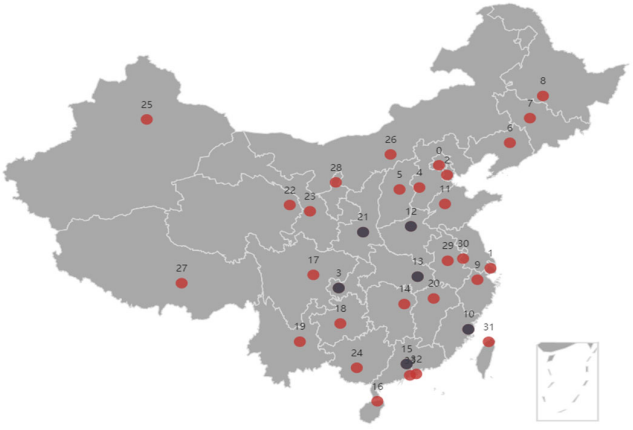

Fig. 3. The distribution of demand nodes and candidate hubs

5.2 Parameters

To bring the case study closer to reality, we draw the experience of the manager with deep backgrounds in the courier industry to help us set parameters, such as the type, capacity, and transportation cost of vehicles and so on. All parameters used are shown in Table 3.

Table 3

Parameter setting

Parameter	Description	Value
N	Set of nodes	China data set
H	Set of candidate hubs	{3,10,12,13,15,21}
w_{ij}	Demand flow from node $i \in N$ to node $j \in N$	China data set
d_{ij}	Distance between nodes $i \in N$ and $j \in N$	China data set
M	Set of vehicle types	$\{a, b\}$
c_a	Transportation cost per kilometer for the ath type vehicle	6 (CNY)
q_a	Capacity of the ath type vehicle	1000 (unit)
mc_a	Monthly fixed cost of the ath type vehicle	20000
c_b	Transportation cost per kilometer for the bth type vehicle	9 (CNY)
q_b	Capacity of the bth type vehicle	5000 (unit)
mc_b	Monthly fixed cost of the bth type vehicle	60000 (CNY)
FH_k	Monthly fixed cost of the kth hub, $k \in H$	700000 (CNY)
FD_i	Monthly fixed cost of the ith node, $i \in N$	300000 (CNY)
lt	Departure time of vehicles when leaving a node	18:00 (h)
dt	The hold time of parcels that must be observed in the hub	12 (h)
s	Service time spent by a vehicle in a hub	0.2 (h)
ε	Unit cost for improving the sorting efficiency of nodes	10 (CNY)
$d\varepsilon$	Unit cost discount for improving the sorting efficiency of hubs	0.8
θ	Unit cost for sorting packages in nodes	0.5(CNY)
$d\theta$	Unit cost discount for sorting packages in hubs	0.8
v	Speed of the vehicle	80 (km/h)
p_c	Preference coefficient of operation costs	0.7
p_t	Preference coefficient of the maximum arrival time	0.3

5.3 Experimental result

In the case of study, the MS-PDM is coded using Python 3.7. The branch-and-cut algorithm of the PB-MOEA is implemented using Gurobi version 9.1.0. In Gurobi, the parameter for gap is set to 0.01%, the parameter for PoolSolutions is set to 100 to determine the retaining number of feasible solutions, and the parameter for PoolGap is set to 10% to obtain feasible solutions within 10% gap of the optimal solution. Besides, the experiments are conducted on a computer with an Intel i5, 2.4 GHz CPU processor, RAM 2.0 GB and Windows 10 OS. In MS-PDM, seven optimization models for designing express transportation networks based on different topologies have been proposed. The PB-MOEA is used to obtain the optimal solution for each model. The calculation method of the gap is shown in (43).

$$Gap = \frac{f_o(s_i) - \min\{F_o\}}{\min\{F_o\}} \qquad \forall s_i \in P, o \in \{1,2\}. \tag{43}$$

The results are shown in Table 4. The first column represents the names of these optimization models. The second column shows the value f_1 of the minimum operation cost (in millions) and the gap between f_1 and the lower bound (in percentage). The third column shows the value f_2 of the maximum arrival time (in hours) and the gap between f_2 and the lower bound (in percentage). The fourth column represents the number of direct links (DL). The fifth column records the computing time (CPU) in seconds. The last column records the selected hubs in the optimal solution.

Table 4

The optimal solution for each model

Models	f_1		f_2		DL	CPU	Hubs
	Million	Gap	Hour	Gap			
FC	124.56	0	44.21	0	1122	1	--
SAHS	113.45	0	80.50	19%	--	681	12,13
MAHS	114.16	0	88.83	0	--	4	3,10,12,13,15,21
RAHS	119.10	0	93.18	16%	--	156	12,13,15
DSAHS	111.17	0	80.54	15%	173	48	13,21
DMAH	109.07	0	88.83	3%	72	5	3,12,13,15,21
DRAHS	110.09	0	72.94	11%	141	58	3,13,21

Table 5 displays the selected hub station and its sorting efficiency of the optimal solution. The second column records the selected hubs in the optimal solution. The third column represent the sorting efficiency of these selected hubs in pieces/hour.

Table 5

The selected hubs and its sorting efficiency for the optimal solution

Models	Hubs	Sorting efficiency (pieces/hour)					
		3	10	12	13	15	21
FC	--	--	--	--	--	--	--
SAHS	12,13	--	--	32109	1072249	--	--
MAHS	3,10,12,13,15,21	16870	118150	177522	233424	519168	39222
RAHS	12,13,15	--	--	92861	615005	396491	--
DSAHS	13,21	--	--	--	254603	--	11327
DMAH	3,12,13,15,21	23617	--	110108	120567	520698	39511
DRAHS	3,13,21	38914	--	--	259954	--	38904

To visualize the network structure of the optimal solutions, we display them in the form of a network diagram in Fig. 4. The red lines indicate the transportation routes opened between the hubs, the yellow lines represent the transportation routes opened between the demand points and the hubs, and the blue lines indicate the direct transportation routes opened between the demand points.

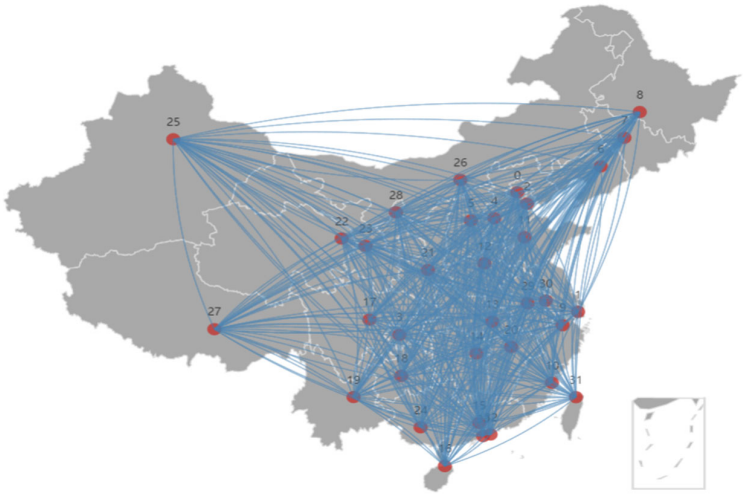

(1) Optimal network structure of FC

(2) Optimal network structure of SAHS

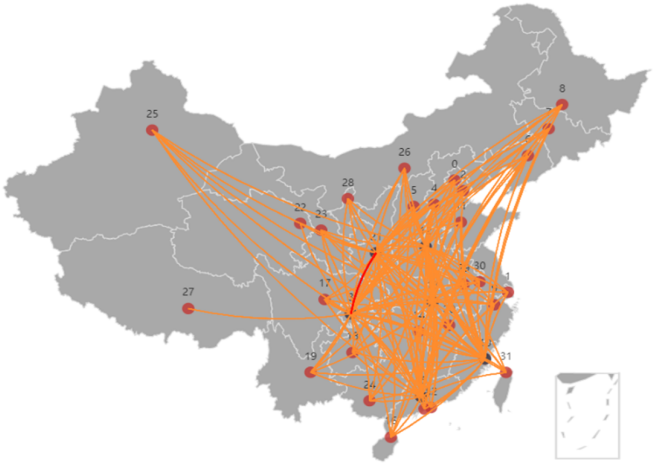

(3) Optimal network structure of MAHS

(4) Optimal network structure of RAHS

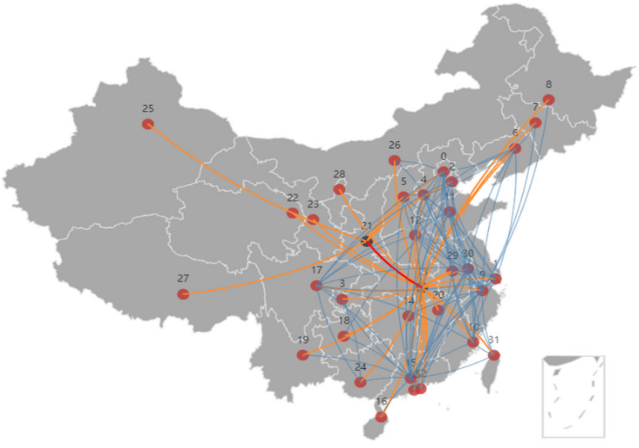

(5) Optimal network structure of DSAHS

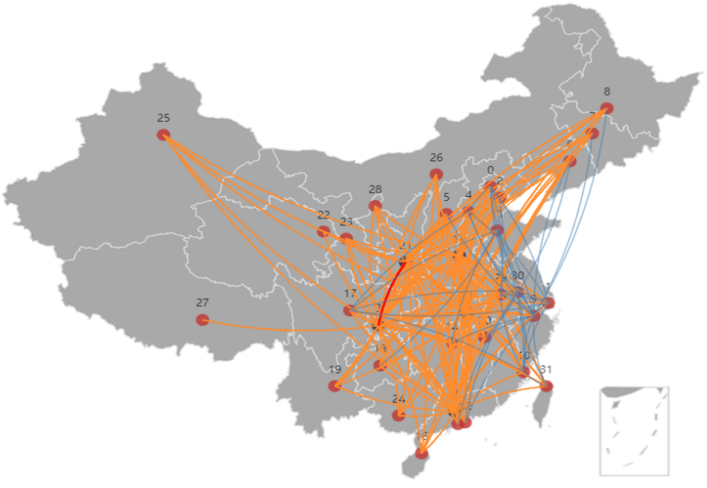

(6) Optimal network structure of DMAHS

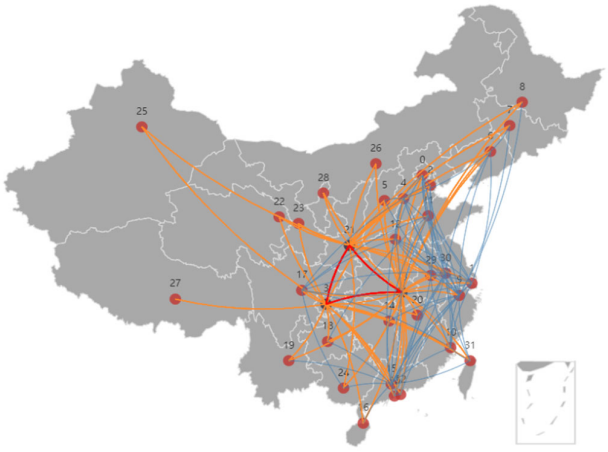

(7) Optimal network structure of DRAHS

Fig. 4. The optimal network structure of ETN under different topologies

As shown in Fig. 4, the performance of these optimal networks varies considerably. We use a scatter plot to show the operation cost and the maximum arrival time in Fig. 5. The optimal network designed based on the FC structure has the best performance in terms of the maximum arrival time, requiring only 44.21 hours, but it also bears the highest operation cost, close to 124.56 million Yuan. Also, the optimal network of the DMAHS has the least operation cost, only 109.07 million Yuan, but the maximum arrival time is close to 90 hours.

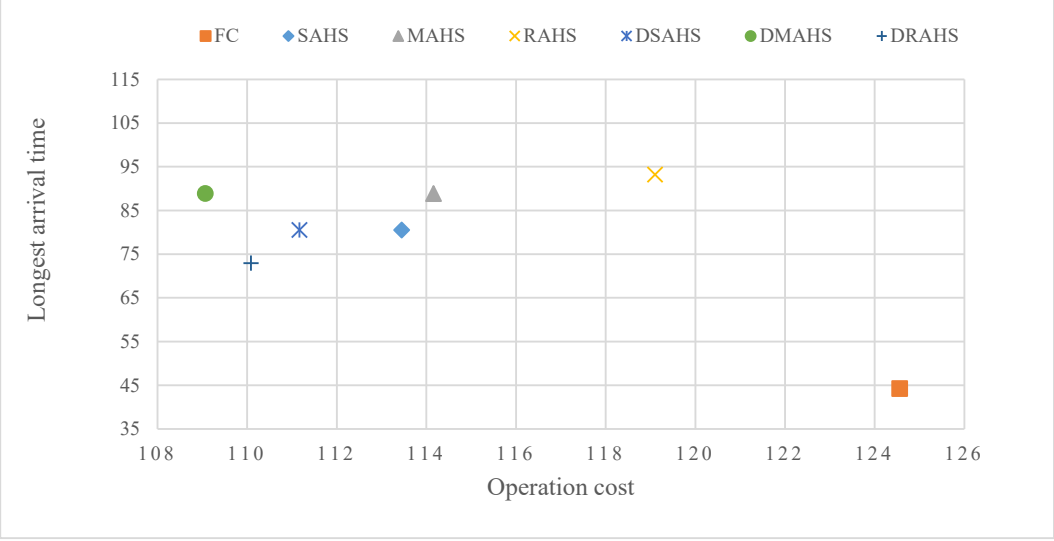

Fig. 5. Performance of these optimal networks

To select the final design solution, we calculate the deviation value F of the decision-maker for each optimal network. The solution with the smallest deviation value of the decision-maker is regarded as the final design solution. The results are shown in Table 6. Following this rule, the optimal network of DRAHS is the final design solution.

Table 6
Decision maker's deviation value of the optimal networks

	FC	SAHS	MAHS	RAHS	DSAHS	DMAHS	DRAHS
F	0.7	0.42	0.50	0.75	0.32	0.27	**0.22**

5.4 Discussion

The values of parameters (q_m, w_{ij}, $d\varepsilon$, $d\theta$, dt) are expected to change with the development of the express industry. To analyze the impact of these parameters on ETNs performance, a series of experiments are conducted in this section to reveal the impact mechanism.

5.4.1 Vehicle capacity

According to the data from the Chinese express company, the vehicle with the largest capacity can transport up to about 5,000 express items per trip. Also, courier companies are trying to use transportation with a larger capacity to transport express items (e.g., trains, high-speed trains, etc.). What impact will this initiative have on ETNs performance?

To this end, we conduct a series of experiments by modifying the maximum capacity of the vehicle. We assume values of the ratios as [1.5, 2, 2.5, 3, 3.5, 4, 4.5, 5]. When the maximum transportation capacity changes, the transportation cost c_b and fixed costs mc_b should also change in the same proportion. The values of these parameters are shown in Table 7.

Table 7
Values of parameters under different capacity ratios

Parameters	**Modifying Ratios**							
	1	**1.5**	**2**	**2.5**	**3.5**	**4**	**4.5**	**5**
q_b	5000	7500	10000	12500	17500	20000	22500	25000
c_b	9	13.5	18	22.5	31.5	36	40.5	45
mc_b	60000	90000	120000	150000	210000	240000	270000	300000

Then, we employ the PB-MOEA algorithm to solve each model under different ratios. The experimental results are shown in Table 8.

Table 8
Performance of optimal solutions under different capacity ratios

Models	**Objective**	**Modifying ratios**								
		1	**1.5**	**2**	**2.5**	**3**	**3.5**	**4**	**4.5**	**5**
FC	f_1	124.56	112.34	106.54	100.47	96.59	93.54	92.83	90.51	90.69
	f_2	44.21	44.21	44.21	44.21	44.21	44.21	44.21	44.21	44.21
SAHS	f_1	113.45	112.78	111.40	105.81	101.09	96.95	93.55	90.84	88.67
	f_2	80.5	71.36	68.11	68.37	68.37	68.52	68.52	68.52	68.52
MAHS	f_1	114.16	113.79	112.31	108.48	105.19	102.43	100.01	97.90	96.08
	f_2	88.83	80.27	74.24	74.25	65.21	65.37	65.02	55.72	55.73
RAHS	f_1	119.1	118.92	114.15	109.69	105.85	102.74	100.06	97.90	96.08
	f_2	93.18	64.70	66.09	74.34	64.74	65.04	65.02	55.73	55.73
DSAHS	f_1	111.17	102.96	94.60	88.70	83.51	79.93	77.46	74.79	72.61
	f_2	80.54	77.55	66.55	66.61	66.47	65.45	75.48	63.50	66.14
DMAHS	f_1	109.07	101.70	93.70	87.85	83.08	79.05	76.03	74.14	71.85
	f_2	88.83	71.49	65.14	65.28	63.81	65.78	65.74	64.27	64.73
DRAHS	f_1	110.09	101.7	93.76	87.86	82.89	79.35	76.54	74.14	71.86
	f_2	72.94	71.49	62.36	65.24	66.02	65.64	65.01	65.66	64.91

The relationship between the capacity and the performance of optimal solutions is shown in Fig. 6 and Fig. 7. It can be seen in Figure 6 that operation costs continue to decrease as the capacity ratio increases. In particular, there is a relatively obvious downward trend in the optimal solutions obtained from the DSAHS, DMAHS, and DRAHS models. In Fig. 7, the change in capacity ratio has no effect on the optimal solution obtained from the FC model. For other models, the maximum arrival time decreases continuously as the capacity ratio increases. However, when the capacity ratio exceeds 2 times, the trend of the maximum arrival time is flat.

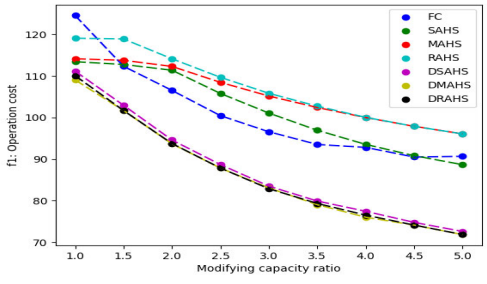

Fig. 6. The impact of capacity on f_1

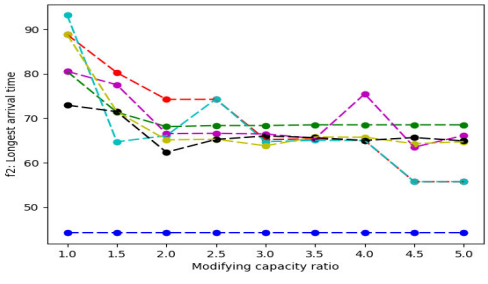

Fig. 7. The impact of capacity on f_2

Therefore, for a courier company, using larger capacity carriers not only helps to save more costs, but also helps to shorten the maximum arrival time.

5.4.2 Demand flow

As the courier market changes, the demand flow from node $i \in N$ to node $j \in N$ may increase or decrease. Therefore, we conduct a series of experiments by adjusting the demand flow. Likewise, we assume that the demand flow between each origin-destination pair varies in proportions of [0.4, 0.6, 0.8, 1, 1.2, 1.4, 1.6]. Then, we use the PB-MOEA algorithm to solve each model at different ratios. The results are shown in Table 9.

Table 9
Performance of optimal solutions under different flow ratios

Models	Objective	Modifying flow ratio						
		0.4	0.6	0.8	1	1.2	1.4	1.6
FC	f_1	69.78	88.09	106.51	124.56	140.48	158.83	175.59
	f_2	44.21	44.21	44.21	44.21	44.21	44.21	44.21
SAHS	f_1	46.36	69.28	91.46	113.45	136.72	159.21	181.71
	f_2	66.64	71.02	77.46	80.5	77.44	77.45	77.44
MAHS	f_1	46.83	69.50	92.18	114.16	137.56	160.24	182.85
	f_2	88.82	88.82	88.82	88.82	88.82	88.82	88.82
RAHS	f_1	48.78	72.64	96.12	119.10	146.97	167.76	190.84
	f_2	90.18	78.04	90.18	93.18	90.18	90.18	90.18
DSAHS	f_1	46.52	68.11	90.50	111.17	133.99	155.38	176.27
	f_2	77.51	77.51	77.52	80.54	77.35	77.41	77.52
DMAHS	f_1	45.08	66.50	88.14	109.07	131.12	152.52	174.32
	f_2	88.82	88.82	88.82	88.82	88.82	88.82	88.82
DRAHS	f_1	46.17	67.32	88.91	110.09	132.10	153.53	175.08
	f_2	65.00	77.51	64.82	72.94	64.77	72.87	77.51

The relationship between the flow and the performance of optimal solutions are shown in Fig. 8 and Fig. 9. Fig. 8 shows that operation costs continue to increase as the flow ratio increases. Notably, when the flow ratio exceeds 1.2 times, the difference in operation cost between the optimal solution obtained from the FC model and other optimal solutions is not significant. However, it can be seen in Fig. 9 that the optimal solution obtained from the FC model performs very well in terms of the maximum arrival time, which is only about 42 hours.

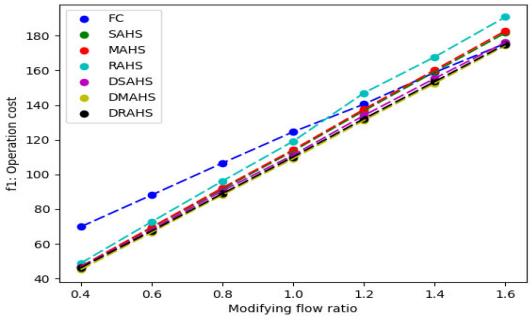

Fig. 8. The impact of flow on f_1

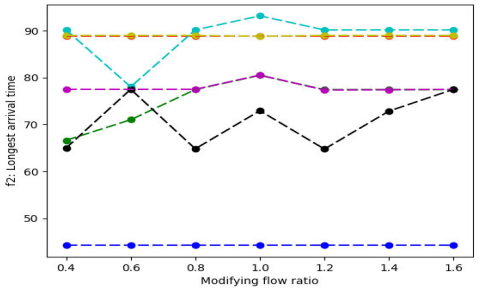

Fig. 9. The impact of flow on f_2

In this scenario, the optimal ETN designed by the FC model performs very well in terms of operating cost and maximum arrival time when the demand traffic increases more than 1.2 times.

5.4.3 Other parameters

In addition, the variation of some parameters, including $d\varepsilon$, $d\theta$, and dt, also has an impact on the network performance. Therefore, we also conduct a series of experiments by modifying the values of these parameters. These parameters are shown in Table 10.

Table 10
Modifying the values of these parameters

Parameters	Case1	Case 2	Case 3	Case 4	Case 5	Case 6	Case 7
$d\varepsilon$	0.2	0.3	0.4	0.5	0.6	0.7	0.8
$d\theta$	0.2	0.3	0.4	0.5	0.6	0.7	0.8
dt	6	8	10	12	14	16	18

Next, we use the PB-MOEA algorithm to solve each model in different cases. The results are shown in Tables 11-13.

Table 11
Performance of optimal solutions for different value of $d\varepsilon$

Models	Objective	$d\varepsilon$						
		0.2	0.3	0.4	0.5	0.6	0.7	0.8
FCC	f_1	124.55	124.55	124.55	124.55	124.55	124.55	124.55
	f_2	44.21	44.21	44.21	44.21	44.21	44.21	44.21
SAHS	f_1	113.11	114.25	114.20	113.56	113.72	114.70	113.45
	f_2	71.27	77.38	77.40	77.45	77.45	77.40	80.5
MAHS	f_1	113.87	114.04	114.21	114.38	114.54	114.70	114.16
	f_2	88.82	88.82	88.82	88.82	88.82	88.82	88.82
RAHS	f_1	119.21	119.38	119.54	119.71	119.87	120.04	119.10
	f_2	78.04	78.04	78.04	78.04	78.04	78.04	93.18
DSAHS	f_1	111.59	111.96	112.06	111.42	111.77	112.11	111.17
	f_2	77.46	77.41	77.36	77.52	77.46	77.52	80.54
DMAHS	f_1	109.16	109.29	109.42	109.55	109.68	109.79	109.07
	f_2	88.82	88.82	88.82	88.82	88.82	88.82	88.82
DRAHS	f_1	110.21	110.67	110.29	110.38	110.41	110.49	110.09
	f_2	77.50	72.78	77.50	64.86	77.50	64.88	72.94

Table 12
Performance of optimal solutions for different value of $d\theta$

Models	Objective	$d\theta$						
		0.2	0.3	0.4	0.5	0.6	0.7	0.8
FC	f_1	124.55	124.55	124.55	124.55	124.55	124.55	124.56
	f_2	44.21	44.21	44.21	44.21	44.21	44.21	44.21
SAHS	f_1	96.26	99.24	102.22	105.20	108.11	111.11	113.45
	f_2	71.18	71.18	77.40	77.40	71.24	71.17	80.5
MAHS	f_1	96.98	99.96	102.94	105.92	108.91	111.89	114.16
	f_2	88.82	88.82	88.82	88.82	88.82	88.82	88.82
RAHS	f_1	102.31	105.30	108.28	111.24	114.24	117.22	119.10
	f_2	78.04	78.04	78.04	78.04	78.04	78.04	78.04
DSAHS	f_1	94.24	97.22	100.20	103.18	106.16	109.15	111.17
	f_2	77.52	77.52	77.52	77.52	77.52	77.52	80.54
DMAHS	f_1	92.02	95.00	97.99	100.97	103.95	106.93	109.07
	f_2	88.82	88.82	88.82	88.82	88.82	88.82	88.82
DRAHS	f_1	92.65	95.63	98.62	101.60	104.58	107.56	110.09
	f_2	64.84	64.84	64.84	64.84	64.84	64.84	72.94

Table 13
Performance of optimal solutions for different value of dt

Models	Objective	dt						
		6	8	10	12	14	16	18
FC	f_1	124.55	124.55	124.55	124.56	124.55	124.55	124.55
	f_2	44.21	44.21	44.21	44.21	44.21	44.21	44.21
SAHS	f_1	116.37	115.54	115.34	113.45	113.87	113.80	114.44
	f_2	69.22	75.43	76.39	80.5	78.45	79.43	73.02
MAHS	f_1	117.02	115.95	115.30	114.16	114.56	114.33	114.15
	f_2	88.82	88.82	88.82	88.82	88.82	88.82	88.82
RAHS	f_1	122.36	121.28	120.64	119.10	119.76	119.55	119.37
	f_2	78.02	78.03	78.04	93.18	92.18	93.18	93.18
DSAHS	f_1	113.34	112.71	112.45	111.17	112.00	111.92	112.15
	f_2	66.33	75.42	68.34	80.54	78.36	79.35	80.21
DMAHS	f_1	111.75	110.80	110.28	109.07	109.65	109.47	109.32
	f_2	88.82	88.82	88.82	88.82	88.82	88.82	88.82
DRAHS	f_1	111.79	111.17	110.80	110.09	110.78	110.20	110.52
	f_2	74.49	64.78	64.81	72.94	78.51	79.51	80.51

To visualize the relationship between these parameters and the performance of optimal solutions, these results are shown in Fig. 10. As can be seen in Fig. 10(a) and Fig. 10(b), the discount rate obtained from the acquisition of sorting equipment at the hubs does not have a significant impact on the operation cost and the maximum arrival time. Fig. 10(c) shows that the higher the discount on parcel sorting costs is, the higher the operation cost is. By contrast, Fig. 10(d) indicates that changes in discount of parcel sorting cost have no noticeable effect on the maximum arrival time. On Figure 10, it can be seen that the longer the hold time of the parcel in the hub, their operation costs have a significant downward trend. However, when the hold time is increased by 12 hours, the operation costs do not have a significant downward trend. In Figure 10-f, we can find that the maximum arrival time increases with the increase in the hold time. In addition, the performance of the optimal solution obtained from the FC model is not affected by these parameters.

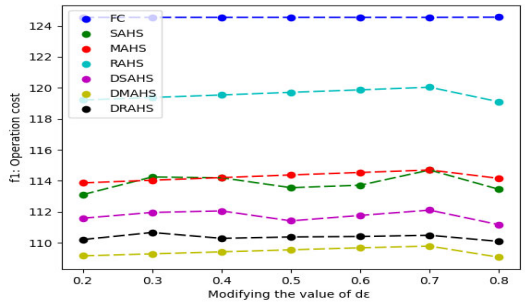

（a）Impact of $d\varepsilon$ on $\boldsymbol{f_1}$

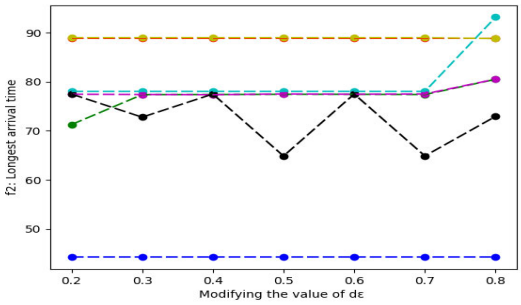

（b）Impact of $d\varepsilon$ on $\boldsymbol{f_2}$

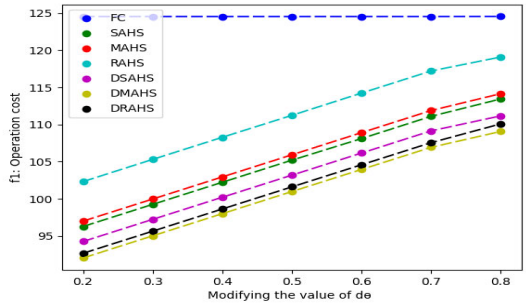

（c）Impact of $d\theta$ on $\boldsymbol{f_1}$

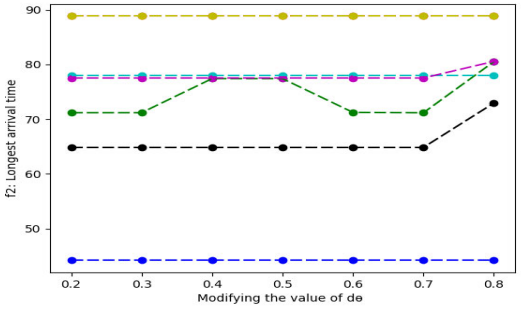

（d）Impact of $d\theta$ on $\boldsymbol{f_2}$

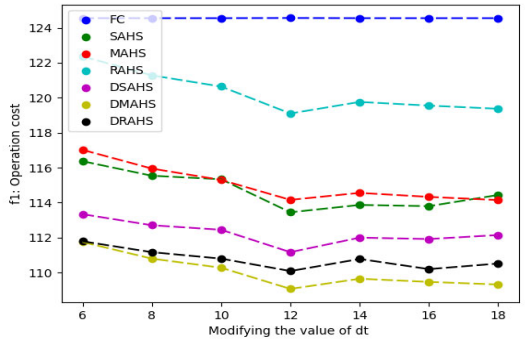

e）Impact of dt on $\boldsymbol{f_1}$

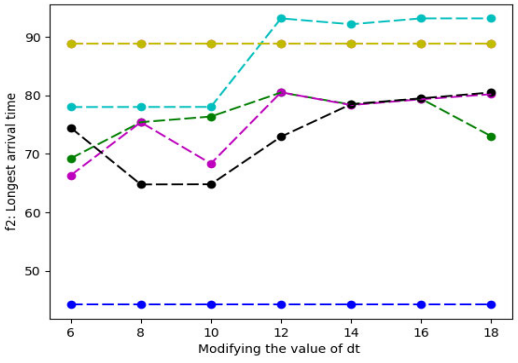

（f）Impact of dt on $\boldsymbol{f_2}$

Fig. 10. The impact of other parameters on the performance of ETN

Therefore, for parameter $d\varepsilon$, if the company puts more effort to obtain a lower discount to improve sorting efficiency, it does not bring significant benefits. However, for parameter $d\theta$, this courier company should consider more ways to reduce the cost of sorting packages, which could result in higher cost savings. For parameter dt, setting a strict hold time for parcels at hubs has no significant impact on the maximum arrival time, but instead pushes up operation costs.

6. Conclusions

In this paper, we propose a multi-structure parallel design methodology to solve BO-ETNDP, which can effectively avoid the limitation of solving BO-ETNDP with a specific structure. In the courier industry, the sorting efficiency of a hub is an important decision variable. Novel bi-objective nonlinear mixed-integer optimization models for BO-ETNDP under multiple structures are developed, which considers the impact of the hub's sorting efficiency on operation cost and arrival time. These models are more in line with the characteristics of the courier industry. To solve these models efficiently, a preference-based multi-objective algorithm (PB-MOA) is devised, which embeds the branch-and-cut algorithm and Pareto dominance theory in the framework of the ranking algorithm. The PB-MOA can obtain high-quality feasible solutions, and accurately measure

its optimality gap. In the case study, the applicability of our methodology is validated in a leading express company. The study also finds that vehicle capacity and demand flow have a significant impact on the structure of ETNs. Also, the applicability scenarios of different topologies in designing ETNs is explored. As future research, we will attempt to extend the BO-ETNDP to consider vehicle scheduling strategies. The models and algorithms involved will be much more complex when vehicle scheduling operations are considered. Another extension is to consider multi-period and traffic uncertainty in the context of BO-ETNDP in order to find the ETN that has the maximum benefit in the coming years.

References

Alumur, S., & Kara, B. Y. (2008). Network hub location problems: The state of the art. *European Journal of Operational Research, 190*(1), 1-21. doi:https://doi.org/10.1016/j.ejor.2007.06.008

Alumur, S. A., Campbell, J. F., Contreras, I., Kara, B. Y., Marianov, V., & O'Kelly, M. E. (2021). Perspectives on modeling hub location problems. *European Journal of Operational Research, 291*(1), 1-17. doi:https://doi.org/10.1016/j.ejor.2020.09.039

An, Y., Zhang, Y., & Zeng, B. (2015). The reliable hub-and-spoke design problem: Models and algorithms. *Transportation Research Part B: Methodological, 77*, 103-122. doi:https://doi.org/10.1016/j.trb.2015.02.006

Aykin, T. (1994). Lagrangian relaxation based approaches to capacitated hub-and-spoke network design problem. *European Journal of Operational Research, 79*(3), 501-523. doi:https://doi.org/10.1016/0377-2217(94)90062-0

Aykin, T. (1995). Networking Policies for Hub-and-Spoke Systems with Application to the Air Transportation System. *Transportation Science, 29*(3), 201-221. doi:10.1287/trsc.29.3.201

Azizi, N., Chauhan, S., Salhi, S., & Vidyarthi, N. (2016). The impact of hub failure in hub-and-spoke networks: Mathematical formulations and solution techniques. *Computers & Operations Research, 65*, 174-188. doi:https://doi.org/10.1016/j.cor.2014.05.012

Batta, R., Lejeune, M., & Prasad, S. (2014). Public facility location using dispersion, population, and equity criteria. *European Journal of Operational Research, 234*(3), 819-829. doi:https://doi.org/10.1016/j.ejor.2013.10.032

Bryan, D. L., & O'Kelly, M. E. (2010). Hub-and-Spoke Networks in Air Transportation: An Analytical Review. *Journal of Regional Science, 39*(2), 275-295.

Campbell, J. F. (1992). Location and allocation for distribution systems with transshipments and transportion economies of scale. *Annals of Operations Research, 40*(1), 77-99. doi:10.1007/BF02060471

da Graça Costa, M., Captivo, M. E., & Clímaco, J. (2008). Capacitated single allocation hub location problem—A bi-criteria approach. *Computers & Operations Research, 35*(11), 3671-3695. doi:10.1016/j.cor.2007.04.005

de Camargo, R. S., de Miranda, G., & Ferreira, R. P. M. (2011). A hybrid Outer-Approximation/Benders Decomposition algorithm for the single allocation hub location problem under congestion. *Operations Research Letters, 39*(5), 329-337. doi:https://doi.org/10.1016/j.orl.2011.06.015

Ebery, J. (2001). Solving large single allocation p-hub problems with two or three hubs. *European Journal of Operational Research, 128*((2)), 447–458.

Erdemir, E. T., Batta, R., Rogerson, P. A., Blatt, A., & Flanigan, M. (2010). Joint ground and air emergency medical services coverage models: A greedy heuristic solution approach. *European Journal of Operational Research, 207*(2), 736-749. doi:https://doi.org/10.1016/j.ejor.2010.05.047

Ernst, A. T., Hamacher, H. , Jiang, H. , Krishnamoorthy, M. , & Woeginger, G. (2009). Uncapacitated single and multiple allocation p -hub center problems. *Computers & Operations Research, 36*(7), 2230–2241.

Esmizadeh, Y., Bashiri, M., Jahani, H., & Almada-Lobo, B. (2021). Cold chain management in hierarchical operational hub networks. *Transportation Research Part E: Logistics and Transportation Review, 147*, 102202. doi:https://doi.org/10.1016/j.tre.2020.102202

Farahani, R. Z., Hekmatfar, M., Arabani, A. B., & Nikbakhsh, E. (2013). Hub location problems: A review of models, classification, solution techniques, and applications. *Computers & Industrial Engineering, 64*(4), 1096-1109. doi:https://doi.org/10.1016/j.cie.2013.01.012

Gelareh, S., & Nickel, S. (2011). Hub location problems in transportation networks. *Transportation Research Part E: Logistics and Transportation Review, 47*(6), 1092-1111. doi:https://doi.org/10.1016/j.tre.2011.04.009

Ghodratnama, A., Tavakkoli-Moghaddam, R., & Azaron, A. (2015). Robust and fuzzy goal programming optimization approaches for a novel multi-objective hub location-allocation problem: A supply chain overview. *Applied Soft Computing, 37*, 255-276. doi:https://doi.org/10.1016/j.asoc.2015.07.038

Hsu, C. I., & Hsieh, Y. P. (2005). Direct versus terminal routing on a maritime hub-and-spoke container network. *Journal of Marine Science and Technology, 13*(3), 209-217.

Hsu, C. I., & Hsieh, Y. P. (2007). Routing, ship size, and sailing frequency decision-making for a maritime hub-and-spoke container network. *Mathematical and Computer Modelling, 45*(7-8), 899-916.

Imai, A., Shintani, K., & Papadimitriou, S. (2009). Multi-port vs. Hub-and-Spoke port calls by containerships. *Transportation Research Part E: Logistics and Transportation Review, 45*(5), 740-757. doi:https://doi.org/10.1016/j.tre.2009.01.002

Karimi-Mamaghan, M., Mohammadi, M., Pirayesh, A., Karimi-Mamaghan, A. M., & Irani, H. (2020). Hub-and-spoke network design under congestion: A learning based metaheuristic. *Transportation Research Part E: Logistics and Transportation Review, 142*, 102069. doi:https://doi.org/10.1016/j.tre.2020.102069

Lin, B., Zhao, Y., & Lin, R. (2020). Optimization for courier delivery service network design based on frequency delay.

Computers & Industrial Engineering, 139, 106144. doi:https://doi.org/10.1016/j.cie.2019.106144

ME, O. K. (1986). Activity levels at hub facilities in interacting networks. *Geogr Anal, 18*, 343–356.

Mohammadi, M., Tavakkoli-Moghaddam, R., Siadat, A., & Rahimi, Y. (2016). A game-based meta-heuristic for a fuzzy bi-objective reliable hub location problem. *Engineering Applications of Artificial Intelligence, 50*, 1-19. doi:https://doi.org/10.1016/j.engappai.2015.12.009

Ng, A. K. Y., & Kee, J. (2008). The optimal ship sizes of container liner feeder services in Southeast Asia: A ship operator's perspective. *Maritime Policy and Management, 35*(4), 353-376. doi:10.1080/03088830802198167

Notteboom, T. E., Parola, F., & Satta, G. (2019). The relationship between transhipment incidence and throughput volatility in North European and Mediterranean container ports. *Journal of Transport Geography, 74*, 371-381. doi:10.1016/j.jtrangeo.2019.01.002

O'Kelly, M. E. (1987). A quadratic integer program for the location of interacting hub facilities. *European Journal of Operational Research, 32*(3), 393-404. doi:https://doi.org/10.1016/S0377-2217(87)80007-3

Real, L. B., Contreras, I., Cordeau, J.-F., de Camargo, R. S., & de Miranda, G. (2021). Multimodal hub network design with flexible routes. *Transportation Research Part E: Logistics and Transportation Review, 146*, 102188. doi:https://doi.org/10.1016/j.tre.2020.102188

Rostami, B., Kämmerling, N., Naoum-Sawaya, J., Buchheim, C., & Clausen, U. (2021). Stochastic single-allocation hub location. *European Journal of Operational Research, 289*(3), 1087-1106. doi:10.1016/j.ejor.2020.07.051

Serper, E. Z., & Alumur, S. A. (2016). The design of capacitated intermodal hub networks with different vehicle types. *Transportation Research Part B: Methodological, 86*, 51-65. doi:https://doi.org/10.1016/j.trb.2016.01.011

Shang, X., Yang, K., Jia, B., Gao, Z., & Ji, H. (2021). Heuristic algorithms for the bi-objective hierarchical multimodal hub location problem in cargo delivery systems. *Applied Mathematical Modelling, 91*, 412-437. doi:10.1016/j.apm.2020.09.057

Sherali, H. D., & Smith, J. C. (2007). An improved linearization strategy for zero-one quadratic programming problems. *Optimization Letters, 1*(1), 33-47. doi:10.1007/s11590-006-0019-0

Skorin-Kapov, D., Skorin-Kapov, J., & O'Kelly, M. (1996). Tight linear programming relaxations of uncapacitated p-hub median problems. *European Journal of Operational Research, 94*(3), 582-593. doi:https://doi.org/10.1016/0377-2217(95)00100-X

Tagawa, H., Kawasaki, T., & Hanaoka, S. (2021). Exploring the factors influencing the cost-effective design of hub-and-spoke and point-to-point networks in maritime transport using a bi-level optimization model. *The Asian Journal of Shipping and Logistics, 37*(2), 192-203. doi:https://doi.org/10.1016/j.ajsl.2021.03.001

Taherkhani, G., & Alumur, S. A. (2019). Profit maximizing hub location problems. *Omega, 86*, 1-15. doi:10.1016/j.omega.2018.05.016

Taslimi, M., Batta, R., & Kwon, C. (2017). A comprehensive modeling framework for hazmat network design, hazmat response team location, and equity of risk. *Computers & Operations Research, 79*, 119-130. doi:https://doi.org/10.1016/j.cor.2016.10.005

Tofighian, A., & Arshadi khamseh, A. (2020). A Bi objective uncapacitated multiple allocation p-hub median problem in public administration considering economies of scales. *Research in Transportation Economics*, 100896. doi:https://doi.org/10.1016/j.retrec.2020.100896

Yaman, H. (2011). Allocation strategies in hub networks. *European Journal of Operational Research, 211*(3), 442-451. doi:https://doi.org/10.1016/j.ejor.2011.01.014

Yaman, H., Kara, B. Y., & Tansel, B. Ç. (2007). The latest arrival hub location problem for cargo delivery systems with stopovers. *Transportation Research Part B: Methodological, 41*(8), 906-919. doi:10.1016/j.trb.2007.03.003

Zahiri, B., & Suresh, N. C. (2021). Hub network design for hazardous-materials transportation under uncertainty. *Transportation Research Part E: Logistics and Transportation Review, 152*, 102424. doi:https://doi.org/10.1016/j.tre.2021.102424